of cladding. Some applications have been presented. For a parabolic-index profile, the results of the rigorous analysis have been shown by which the present theory has been verified.

APPENDIX

Derivation of (31) is as follows:

$$\begin{aligned}\Phi_{n1}'(x_c) &+ k\sqrt{\chi_1(x_c) - b_{n1}}\,\Phi_{n1}(x_c)\\ &= [dy/dx]^{1/2}\{\Phi_{n0}'(y_c) - [y''(x_c)/2y'^2(x_c)]\Phi_{n0}(y_c)\\ &\quad + (dy/dx)^{-1}k\sqrt{\chi_1(x_c) - b_{n1}}\,\Phi_{n0}(y_c)\}\\ &= [dy/dx]^{1/2}\{\Phi_{n0}'(y_c) + k\sqrt{\chi_0(y_c) - b_{n0}}\,\Phi_{n0}(y_c)\\ &\quad - [y''(x_c)/2y'^2(x_c)]\Phi_{n0}(y_c)\}\\ &\simeq [dy/dx]^{1/2}\{\Phi_{n0}'(y_c) + k\sqrt{\chi_0(y_c) - b_{n0}}\,\Phi_{n0}(y_c)\}.\end{aligned}$$

Similarly, we obtain

$$\begin{aligned}\Psi_{n1}'(x_c) &+ k\sqrt{\chi_1(x_c) - b_{n1}}\,\Psi_{n1}(x_c)\\ &\simeq [dy/dx]^{1/2}\{\Psi_{n0}'(y_c) + k\sqrt{\chi_0(y_c) - b_{n0}}\,\Psi_{n0}(y_c)\}.\end{aligned}$$

Substituting these results into (17), we obtain (31).

ACKNOWLEDGMENT

The author wishes to thank the Editor and the reviewers for recommending the publication of this work as a paper instead of as a Letter.

REFERENCES

[1] For example, M. O. Vassel, "Calculation of propagating modes in a graded-index optical fiber," *Opt-Electron.*, vol. 6, pp. 271–286, 1974.
[2] M. Hashimoto, "The effect of an outer layer on propagation in a parabolic-index optical waveguide," *Int. J. Electron.*, vol. 39, no. 5, pp. 579–582, 1975.
[3] H. A. Kramers, "Wellenmechanik und halbzahlige Quantisierung," *Z. Physik*, vol. 39, pp. 828–840, 1926.
[4] M. Hashimoto, "Eddy power flow of electromagnetic waves," *Int. J. Electron.*, vol. 34, no. 5, pp. 713–716, 1973.
[5] H. W. Bode, *Network Analysis and Feedback Amplifier Design.* New Jersey: van Nostrand, 1945.
[6] D. Marcuse, *Light Transmission Optics.* New York: van Nostrand, 1972.
[7] S. Moriguchi, K. Udagawa, and S. Hitotsumatsu, *Mathematical Formulas III* (in Japanese). Tokyo: Iwanami, 1972, p. 94.
[8] E. T. Whittaker and G. N. Watson, *A Course of Modern Analysis.* London: Cambridge, 1963.
[9] A. Erdèlyi, W. Magnus, F. Oberhettinger, and F. G. Tricomi, *Higher Transcendental Functions*, vol. II. New York: McGraw-Hill, 1953.
[10] M. Hashimoto, "A perturbation method for the analysis of wave propagation in inhomogeneous dielectric waveguides with perturbed media," *IEEE Trans. MTT*, to be published.

Fringing-Field Effects in Edge-Guided Wave Devices

PIETRO DE SANTIS, MEMBER, IEEE

***Abstract*—An equivalent model is presented for evaluating the fringing-field effects in edge-guided waves (EGW) propagating along ferrite microstrip circuits. It is based on the approximate model developed by Getsinger for nonferromagnetic microstrip circuits. Fringing-field effects are characterized by a fringing-field parameter b/b' whose numerical value is determined by experiment. Measurements are made on EGW resonators of various shapes for different values of the applied magnetic bias.**

Finally, the fringing-field parameter is used to evaluate the ratio between the reactive power stored in the fringing fields and the RF power in the ferrite under the strip conductor in a disk resonator.

I. INTRODUCTION

FRINGING-FIELD effects in ferrite microstrips have been studied by a number of authors [1]–[3]. Similar to what has been done for microstrips on a nonmagnetic substrate, they are accounted for by introducing a "magnetic" filling factor, which reduces the numerical value of the magnetic permeability of the substrate. Therefore, in ferrite microstrip lines both the dielectric permittivity and the magnetic permeability of the substrate's material have "effective" values. In general they are given in the form

$$\varepsilon_{\text{eff}} = 1 + q_e(\varepsilon_r - 1) \tag{1}$$

$$\mu_{\text{eff}} = \left[1 + q_m\left(\frac{1}{\mu_r} - 1\right)\right]^{-1} \tag{2}$$

where q_e and q_m are the electric and magnetic filling factors, ε_r and μ_r are the relative dielectric permittivity and magnetic permeability of the substrate. The two quantities q_e and q_m depend upon the geometry of the microstrip circuit and are in general different from each other [4].

The expressions (1) and (2) are valid under the hypothesis that the substrate is characterized by scalar constitutive

Manuscript received August 11, 1975; revised December 29, 1975.
The author is with the Research Department, Selenia S.p.A., Via Tiburtina Km. 12,400, 00131 Rome, Italy.

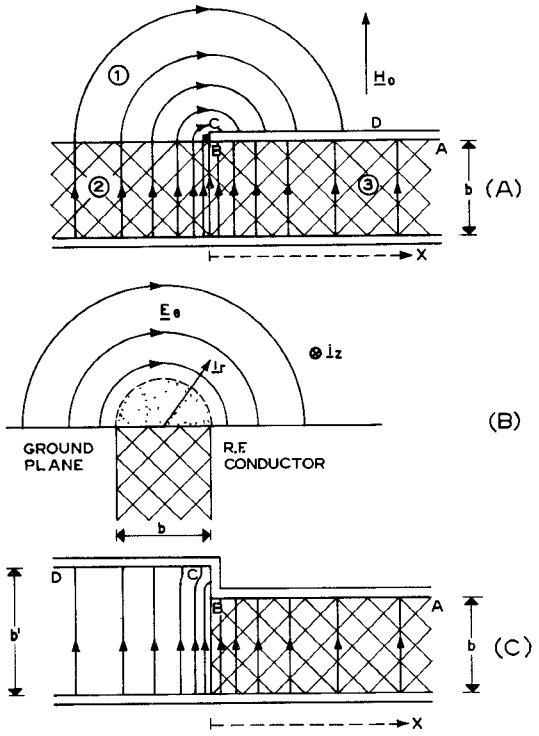

Fig. 1. (a) Pictorial representation of the fringing fields of an EGW in the TEM approximation [6]. (b) Equivalent model used to evaluate the fringing-field admittance at $X = 0$, [7]. (c) Proposed equivalent model.

parameters and the electromagnetic field extends throughout the volume between the ground plane and the strip conductor, i.e., it is a "volume wave" field.

Whenever this volume wave field propagates in a wide microstrip ($W/b \gg 1$, W being the strip's width and b the substrate's thickness) the use of (1) and (2) in conjunction with perfect magnetic-wall boundary conditions at the strip's edges, yields a good agreement between theory and experiment [5]. Under these circumstances most of the guided power flows under the strip conductor and only a small fraction of it is involved in the fringing fields. A different situation may be encountered in wide ferrite microstrips magnetized perpendicularly to the ground plane.

Here the RF fields may be concentrated at one strip's edge and their amplitudes decrease toward the axis of the structure [edge-guided wave (EGW)]. A pictorial representation of an EGW field was given by Hines in [6] and is repeated in Fig. 1(a).

In this figure one may recognize that, even in a very wide microstrip, the fringing-field power in regions 1 and 2 is a significant portion of the total EGW power whenever the field's amplitude in region 3 displays a rapid transversal attenuation.

We have obtained experimental evidence that in wide ferrite microstrips RF fields of considerable amplitude exist in the air just above the ferrite substrate outside the strip conductor. Fig. 2 shows the vertical component of the electric field measured by a coaxial probe scanned in

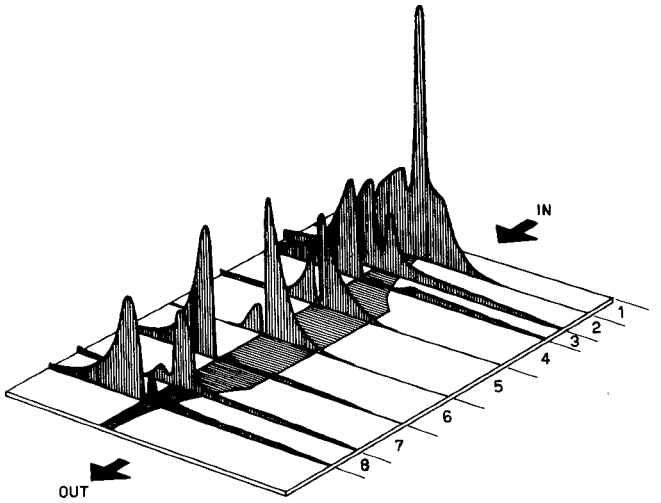

Fig. 2. Spatial distribution of the vertical component of the electric field in an EGW circuit. Operation frequency: 8.3 GHz, $H_0 = 3100$ Oe. The substrate is YIG, 0.6 × 36 × 50.8 mm. The central part of the strip is 6.4 mm wide.

planes perpendicular to the microstrip axis. The substrate is a YIG plate 0.6 × 36 × 50.8 mm, the central part of the strip conductor is 6.4 mm wide, the operation frequency is 8.3 GHz, and the magnetic bias $H_0 = 3100$ Oe. In Fig. 2 a number of interesting phenomena are evident, such as a longitudinal stationarity, a strong transversal-field displacement effect, and the presence of RF fields at one of the substrate's edges. All these phenomena are of no easy interpretation in terms of pure EGW propagation. Probably surface wave propagation and scattering from the metallic probe are present as well. Although no clean excitation of a pure EGW mode was possible, however, it seems reasonable to associate the transversal-field displacement effect with an EGW phenomenon. Therefore, we conclude that qualitative experimental evidence exists of the presence of EGW fringing fields in the air just above the substrate surface. A quantitative evaluation of the fringing-field power, however, is not possible unless suitable steps are taken to avoid the simultaneous excitation of spurious modes.

In [7] the fringing field effects were theoretically evaluated by introducing an "edge admittance" which was calculated by means of an equivalent model. The model is shown in Fig. 1(b) and is derived from the original structure by conformal mapping techniques. The edge admittance $Y = H_y(0)/E_z(0)$ at $x = 0$ [Fig. 1(a)] was obtained from the model of Fig. 1(b) by neglecting the RF fields in the $r < (b/2)$ region (shaded area) and imposing

$$bE_z(0) = \frac{\pi}{2} bE_\theta\left(\frac{b}{2}\right)$$

$$H_y(0) = H_z\left(\frac{b}{2}\right). \tag{3}$$

Here the quantities on the right- and left-hand side, respectively, refer to the model and to the original structure. The resolution of the boundary value problem relative to

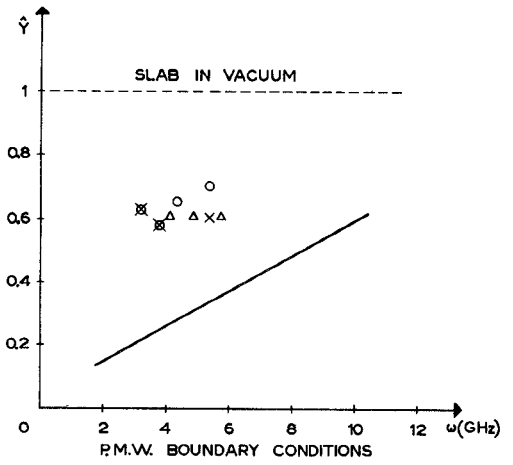

Fig. 3. The normalized edge admittance defined in [7] as a function of frequency. Data points refer to the EGW resonators of Fig. 5.

the model [7] enables one to calculate E_θ and H_z and finally to obtain

$$Y = \frac{jK_a}{\omega\mu_0} \cdot \frac{\pi}{2} \cdot \frac{K_0\left(K_a \frac{b}{2}\right)}{K_1\left(K_a \frac{b}{2}\right)}. \tag{4}$$

Here K_a is the radial wavenumber in air, ω is the operation radian frequency, μ_0 the absolute magnetic permeability of vacuum, and K_0 and K_1 the modified Bessel's functions of the second kind.

The formula (4) completely characterizes the fringing-field effects once K_a is determined. This implies the computer solution of the trascendental equation obtained by equating (4) to the transversal wave admittance at $x = 0^+$. This was, in fact, done in [7]. From the data reported in [7] for a semi-infinite microstrip deposited on a YIG substrate 0.025 in thick, immersed in a dc magnetic field $H_0 = 1780$ Oe, we have calculated the normalized edge admittance $\hat{Y} = Y(\omega\mu_0/K_a)$ as a function of frequency. This is shown by a solid line in Fig. 3. This figure shows that the model predicts a normalized edge admittance which increases from values close to the perfect magnetic-wall boundary condition ($\hat{Y} = 0$) toward values close to the "slab in vacuum" situation ($\hat{Y} = 1$). In Fig. 3 we have also shown some experimental results obtained by observing EGW resonances in MIC resonators of various shapes (see Section III). Unfortunately, the agreement between theory and experiment is rather poor.

At this point one might think of introducing a more sophisticated model which would produce a better agreement between theory and experiment. This process, however, would inevitably lead to major analytical complexities which on the other hand would not eliminate the need of checking the results by experiment. In the light of these considerations we suggest the use of a very simple equivalent model and recognize from the very beginning that the analysis must have a semi-empirical character, i.e., it must contain an adjustable parameter to be determined by experiment.

The difficulty of the problem is now represented by the choice and determination of such a parameter. As a first choice one might select the edge admittance itself as a parameter and measure it. Another possibility is to look at the methods of evaluating fringing-field effects in isotropic microstrips and extend them to the case under consideration. We have chosen the latter possibility and, more specifically, we have applied Getsinger's analysis [8] to the case of EGW propagation.

In the following section it will be shown that the empirical parameter introduced by Getsinger for nonferromagnetic microstrips is suitable also for ferrite microstrips and can be related to the edge admittance in a very simple manner.

II. The Equivalent Model

A simplified model equivalent to the original EGW microstrip circuit of Fig. 1(a) is found following the lines of Getsinger's analysis [8]. It is obtained by deforming the geometry of Fig. 1(a) as shown in Fig. 1(c) and is constituted by two parallel-plane waveguides of heights b and b', respectively, filled with ferrite and air, joined together at $x = 0$. As in Getsinger's analysis the junction effects at $x = 0$ are neglected because they greatly complicate the analysis and are not found necessary for practical results.

If the applied dc magnetic field $\boldsymbol{H}_0$ is parallel to the Z axis and Z-independent RF fields are considered, the modes separate into TE_z and TM_z, and only the latter are affected by the magnetic anisotropy of the ferrite. In fact they propagate in a medium of effective magnetic permeability $\mu_{\text{eff}} = (\mu_1^2 - \mu_2^2)/\mu_1$ where μ_1 and μ_2 are the usual components of Polder's tensor. Assuming a dependence $e^{[j(\omega t - K_y y)]}$ for all fields quantities one finds that for $x < 0$

$$\frac{d^2E_{za}}{dx^2} - K_{xa}^2 E_{za} = 0 \tag{5}$$

$$E_{za}(x) = Ae^{K_{xa}x}, \qquad (K_{xa} > 0) \tag{6}$$

$$H_{ya}(x) = \frac{-jK_{xa}}{\omega\mu_0} Ae^{K_{xa}x} \tag{7}$$

$$K_y^2 - K_{xa}^2 = \omega^2\varepsilon_0\mu_0 = K_0^2 \tag{8}$$

and for $x > 0$

$$\frac{d^2E_{zf}}{dx^2} - K_{xf}^2 E_{zf} = 0 \tag{9}$$

$$E_{zf}(x) = Be^{-K_{xf}x}, \qquad (K_{xf} > 0) \tag{10}$$

$$H_{yf}(x) = \frac{jB}{\omega\mu_0\mu_{\text{eff}}}\left(K_{xf} - \frac{\mu_2}{\mu_1}K_y\right)e^{-K_{xf}x} \tag{11}$$

$$K_y^2 - K_{xf}^2 = \omega^2\varepsilon_0\mu_0\varepsilon_f\mu_{\text{eff}} = K_f^2\mu_{\text{eff}} \tag{12}$$

where ε_f is the relative dielectric constant of the ferrite and A,B are amplitude constants.

To find the characteristic equation of the model, let us introduce two equivalent transmission lines, respectively, extending along the positive and negative X axis, and

associate with them the characteristic admittances [9],

$$\vec{Y}_f = \frac{\int_0^1 \int_0^b (\boldsymbol{E}_{zf} \times \boldsymbol{H}_{yf}^* \cdot \boldsymbol{i}_x)\, dy\, dz}{|E_{zf}|^2 b^2} \tag{13}$$

$$\overleftarrow{Y}_a = \frac{\int_0^1 \int_0^{b'} [\boldsymbol{E}_{za} \times \boldsymbol{H}_{ya}^* \cdot (-\boldsymbol{i}_x)]\, dy\, dz}{|E_{za}|^2 (b')^2} \tag{14}$$

where $\boldsymbol{i}_x$ is the unit vector in the x direction, and the asterisk indicates the complex conjugate.

Note that Y_f and Y_a are x-independent quantities. Let us now impose the matching condition

$$\overleftarrow{Y}_a + \vec{Y}_f = 0 \tag{15}$$

and, via (6), (7)–(10), (11) and (13), (14) obtain

$$K_{xf} - \frac{\mu_2}{\mu_1} K_y + \mu_{\text{eff}} \frac{b}{b'} K_{xa} = 0. \tag{16}$$

This is the characteristic equation of the model, the junction effects at $x = 0$ being neglected.

Here b/b' plays the same formal role as in Getsinger's analysis [8, eq. 8]. However, at variance to the isotropic case, b/b' is now a function of the magnetic properties of the substrate. In general, for an EGW microstrip circuit of thickness b and radius of curvature R, one would expect $(b/b') = (b/b')[R,b,(\omega/\omega_0),(\omega/\omega_m),\varepsilon_f]$ where $\omega_0 = \gamma H_0$, $\omega_m = \gamma 4\pi M_S$, γ being the electron gyromagnetic ratio and $4\pi M_S$ the saturation magnetization of the ferrite.

In the following section we shall present the experimental determination of (b/b') for various MIC circuits with different magnetic biases.

III. The Determination of b/b'

The determination of the numerical values of b/b' was made by observing EGW resonances in ferrite MIC resonators of various shapes with different magnetic biases. Disk resonators, "circular-hole" resonators wherein the substrate is metallized everywhere but in a disk-shaped region and resonators with mixed rectilinear and circular edges were tested. The geometrical dimensions of each resonator are reported in Table I. Note that the radius of curvature of the circular-hole resonator is opposite in sign to that of the disk resonator and that in the resonators 3) and 4) the length of the rectilinear guiding edge is, respectively, 17.5 and 39 percent of the total length. Therefore, the measurement of resonances in these resonators may provide helpful information on how the curvature radius of the guiding edge influences the EGW propagation. EGW disk resonators were already studied in [10] and here we just report the guidelines of the analysis.

In a MIC disk, deposited on a ferrite substrate magnetized perpendicularly to the ground plane, EGW's exist when $\mu_{\text{eff}} < 0$. They are undirectional waves, i.e., they circulate in a given sense of propagation for a given orientation of the applied magnetic bias $\boldsymbol{H}_0$. If the RF signal is injected into and extracted from the resonator by lightly coupled microstrip lines (miniature coaxial probes for the circular-hole resonator), resonances are expected in the transmission

TABLE I
Geometrical Characteristics of the EGW Resonators Shown in the Insert of Fig. 5

Type of resonato	h (*)	R	ΔK_y (rad/m)
1) Disk	-	15	66.66
2) Circular hole	-	15	66.66
3) Rectilinear + Circular	10	15	54.99
4) Rectilinear + Circular	20	10	61.09

(*) All lengths are in mm.

Note: From left to right, the vertical columns indicate 1) the length of the rectilinear portion; 2) the curvature radius of the circular edge; 3) $\Delta K_y = 2\pi/L$, the increase in longitudinal wavenumber between two successive resonances. L is the total length of the guiding edge.

spectrum whenever the azimuthal index is an integer, i.e.,

$$n = K_\theta R = m, \qquad m = 1,2,3,\cdots \tag{17}$$

where R is the radius of the disk and K_θ an azimuthal wavenumber which reduces to K_y for $R \to \infty$.

As it is common practice in this type of experiment, the radius of the circular edges is chosen sufficiently large to neglect curvature effects, i.e., $K_\theta \simeq K_y$ [11]. A similar type of reasoning is believed to be valid in principle for the other EGW resonators. Swept-frequency measurements from 2 to 12.5 GHz were made of the transmission spectrum of the resonators for $H_0 = 2$, 3, 4 kOe. Each resonance frequency was associated to a discrete value of K_y corresponding to $(2m\pi/L)$, L being the length of the guiding edge (see the third column in Table I).

The data points were superimposed on the dispersion curves of the equivalent model, drawn on a frequency versus K_y coordinate plane. Each dispersion curve was numerically calculated from (16), with b/b' as a constant parameter. In Figs. 4–6, H_0 is, respectively, equal to 2, 3, and 4 kOe, while the values of b/b' cover the range of interest 0–1. From these results it is concluded that in many cases of interest b/b' lies between 0.4 and 0.7, i.e., between the perfect magnetic wall $[b/b' = 0]$ and the slab in vacuum $[b/b' = 1]$ limits. In Figs. 4–6 we have also indicated with dotted lines the dispersion curves relative to the edge admittance given by formula (4). Unfortunately, the agreement between these curves and the experimental points is in general rather poor.

Finally, we note that the knowledge of the numerical value of b/b' has a twofold importance: it provides the correct behavior of the dispersion curves of the EGW circuit and the exact value of the edge admittance at the strip's edge. In particular, the knowledge of the edge admittance is of practical importance as it permits one to calculate the reactive power stored in the fringing fields

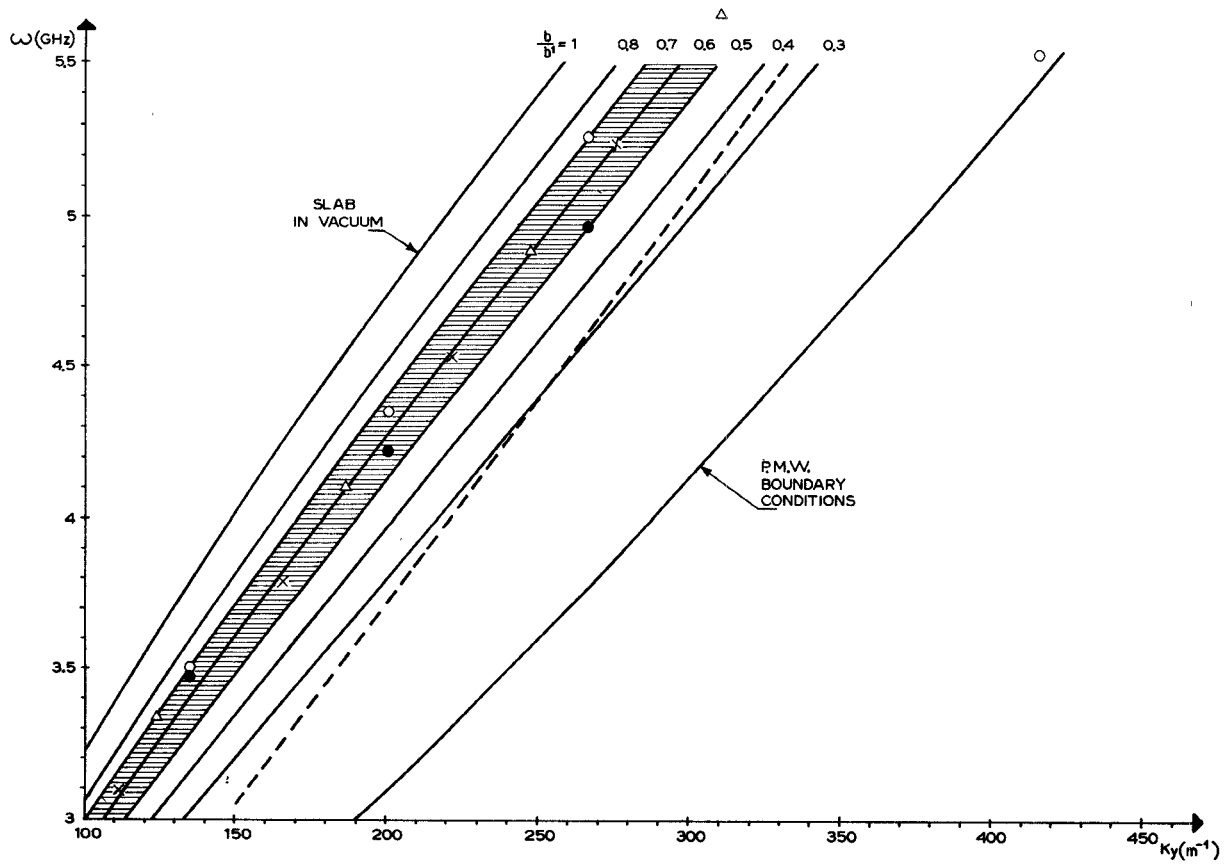

Fig. 4. Dispersion curves as calculated from (16). $4\pi M_s = 1780$ Oe, $H_0 = 2000$ Oe. Data points refer to the EGW resonators in the insert of Fig. 5. The dotted line was calculated using formula (4) for the edge admittance.

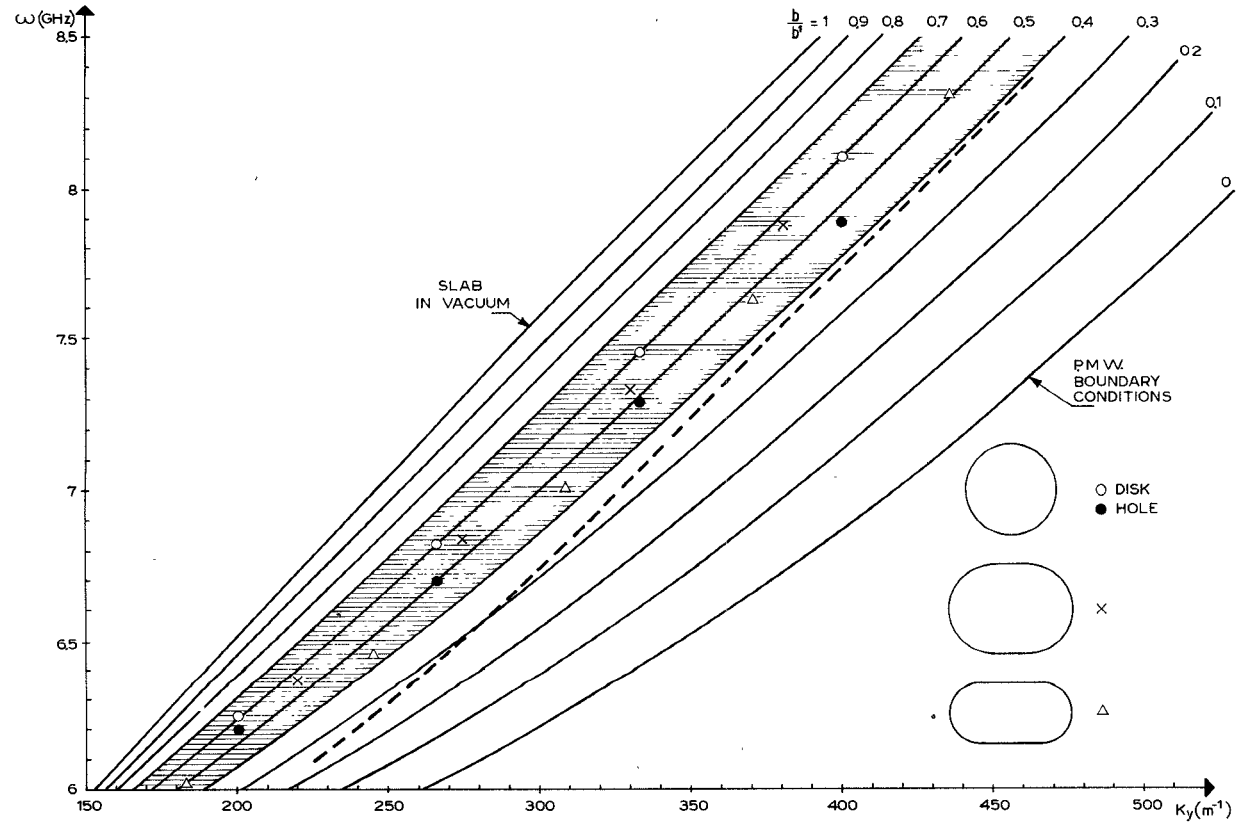

Fig. 5. Same as Fig. 4. $H_0 = 3000$ Oe.

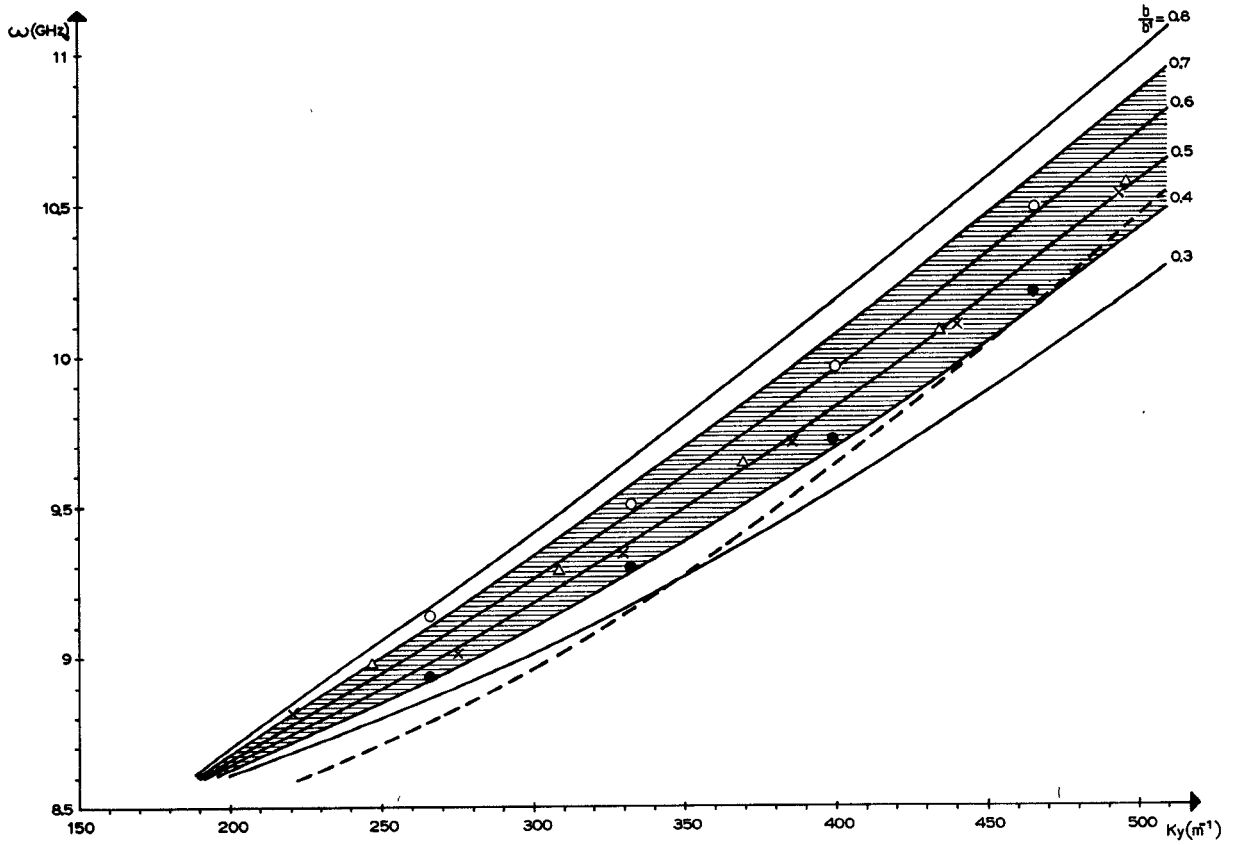

Fig. 6. Same as Fig. 5. $H_0 = 4000$ Oe.

as well as to evaluate a "compensative" loading of the guiding edge [7]. The explicit relation between the edge admittance and the parameter b/b' is given in the following section.

IV. Fringing-Field Power

In Section III fringing-field effects were characterized by an adimensional parameter b/b' whose numerical value was determined by experiment.

In this section we shall use b/b' to calculate the ratio between the reactive power P_a stored in the fringing fields and the RF power P_f under the strip conductor in an EGW disk resonator of thickness b and circumference length L. In the spirit of the measurements described in Section III, curvature effects are neglected and reference is made to a rectilinear geometry.

Under these circumstances the reactive power stored in the fringing fields is

$$P_a = \tfrac{1}{2}|Y_e||E_{zf}(0)|^2 b^2 \tag{18}$$

where Y_e is the edge admittance as seen from inside a rectilinear microstrip of height b and length L (see the insert of Fig. 7).

To find the relation between $|Y_e|$ and b/b', refer to (13), and obtain

$$\int_0^L \int_0^b E_{zf} H_{yf}^* \, dy \, dz = Y_e |E_{zf}|^2 b^2 \tag{19}$$

or via (10), (11)

$$K_{xf} - \frac{\mu_2}{\mu_1} K_y - jY_e \frac{b}{L} \omega \mu_0 \mu_{\text{eff}} = 0. \tag{20}$$

A comparison of this equation with (16) yields the relation

$$Y_e = j \frac{L}{b} \frac{b}{b'} \frac{K_{xa}}{\omega \mu_0}. \tag{21}$$

The net reactive power stored under the strip conductor is

$$P_f = \frac{\omega}{2} \left\{ \int_0^\infty \int_0^L \int_0^b \left[\mu_0 \frac{\partial(\omega \mu_{\text{eff}})}{\partial \omega} (|H_{xf}|^2 + |H_{yf}|^2) - \varepsilon_0 \varepsilon_f |E_{zf}|^2 \right] dx \, dy \, dz \right\}. \tag{22}$$

Substitution of (10) and (11) into (22), and (10) and (21) into (18) leads to

$$\frac{P_a}{P_f} = \frac{2 \frac{b}{b'} K_{xa} K_{xf} \mu_{\text{eff}}}{\left\{ \left[1 + \left(\frac{\mu_2}{\mu_1} \right)^2 \right] (K_{xf}^2 + K_y^2) - \frac{4\mu_2}{\mu_1} K_{xf} K_y \right\} \cdot \left(1 + \frac{\omega}{\mu_{\text{eff}}} \frac{\partial \mu_{\text{eff}}}{\partial \omega} \right) - K_0^2 \varepsilon_f \mu_{\text{eff}}}. \tag{23}$$

Fig. 7 shows the numerical solution of (23) for an EGW disk resonator of radius 15 mm, deposited on a substrate 0.6 mm thick, immersed in dc magnetic fields of 2, 3, 4 kOe.

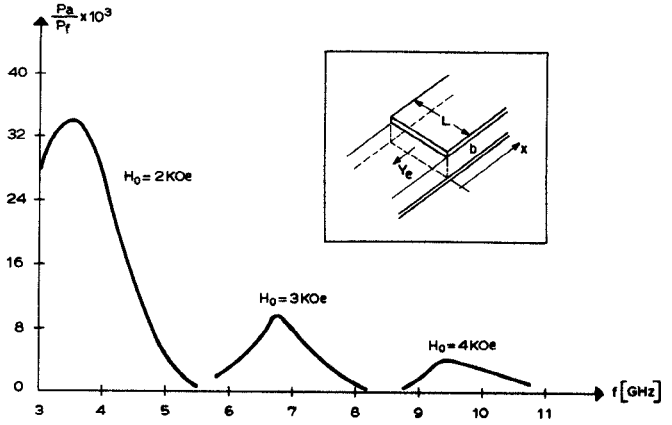

Fig. 7. The ratio of the fringing-field power and the RF power stored in the ferrite under the strip conductor. All values are multiplied by 1000.

The dispersion characteristics of this resonator were studied in Section III and reported in Figs. 4–6 (open circles). From Fig. 7 it appears that in an EGW resonator with $b/L = 0.0063$ the ratio between the reactive power stored in the fringing fields and the total RF power under the strip conductor is within the range 10^{-2}–10^{-3} as H_0 increases from 2 to 4 kOe. Note that the previous procedure is applicable also to the evaluation of reactive power stored in the fringing fields of conventional MIC disk resonators such as used in MIC junction circulators.

V. Conclusions

A simplified equivalent model is proposed to evaluate fringing-field effects in ferrite microstrip circuits excited on the EGW mode. It is found that, similar to what has been done by Getsinger for nonferromagnetic microstrip circuits, an empirical parameter can be introduced into the analysis to provide good dispersion curves for many cases of practical interest. Measurements on EGW resonators of various shapes and with different magnetic biases were made for the determination of such a parameter. It was found that a numerical value between 0.4 and 0.7 is appropriate for most cases.

In the last section a relation is found between the fringing-field parameter and the edge admittance necessary to calculate the reactive power stored in the fringing fields. It is found that in an EGW disk resonator with an aspect ratio $b/L = 0.0063$, the ratio between the fringing-field power and the RF power under the strip conductor is of the order of a few percent.

Acknowledgment

The author wishes to thank Dr. G. Cortucci and Dr. F. Marcelja for the numerical evaluation of the dispersion curves, Dr. C. Misiano for constructing the MIC circuits, and F. Pucci for the measurements on the resonators. He also wishes to thank Prof. F. J. Rosenbaum for some enlightening discussions relative to Section IV.

References

[1] G. T. Roome and H. A. Hair, "Thin ferrite devices for microwave integrated circuits," *IEEE Trans. on Microwave Theory and Techniques*, vol. MTT-16, pp. 411–420, July 1968.
[2] T. Kaneki, "Analysis of linear microstrip using an arbitrary ferromagnetic substance as the substrate," *Electr. Letters*, vol. 5, pp. 465–466, Sept. 18, 1969.
[3] R. A. Pucel and D. J. Massé, "Microstrip propagation on magnetic substrates. Part I: Design theory," *IEEE Trans. on Microwave Theory and Techniques*, vol. MTT-20, pp. 307–313, May 1972.
[4] F. J. Rosenbaum, "Integrated ferrimagnetic devices," in *Advances in Microwaves*. New York: Academic Press, 1974, pp. 203–294.
[5] Y. S. Wu and F. J. Rosenbaum, "Mode chart for microstrip ring resonators," *IEEE Trans. on Microwave Theory and Techniques*, vol. MTT-22, pp. 487–489, July 1973.
[6] M. E. Hines, "A new microstrip isolator and its application to distributed diode amplification," *IEEE G-MTT 1970 Microwave Symposium, Papers' Digest*, pp. 304–307.
[7] ——, "Reciprocal and nonreciprocal modes of propagation in ferrite striplines and microstrip devices," *IEEE Trans. on Microwave Theory and Techniques*, vol. MTT-19, pp. 442–451, May 1971.
[8] W. J. Getsinger, "Microstrip dispersion model," *IEEE Trans. on Microwave Theory and Techniques*, vol. MTT-21, pp. 34–39, Jan. 1973.
[9] J. A. Schelkunoff, *Electromagnetic Waves*. New York: Van Nostrand Co., 1943, p. 319.
[10] P. de Santis, "Edge-guided modes in ferrite microstrip with curved edges," *Applied Physics*, vol. 4, pp. 167–174, April 1974.
[11] P. Troughton, "Measurement techniques in microstrip," *Electron. Lett.*, vol. 5, pp. 25–26, Jan. 1969.